Redefinition of satimolite

Igor V. Pekov[1,*], Natalia V. Zubkova[1], Dmitry A. Ksenofontov[1], Nikita V. Chukanov[2], Vasiliy O. Yapaskurt[1], Oksana V. Korotchenkova[3], Ilya I. Chaikovskiy[3], Vladimir M. Bocharov[4,†], Sergey N. Britvin[5] and Dmitry Yu. Pushcharovsky[1]

[1] Faculty of Geology, Moscow State University, Vorobievy Gory, 119991 Moscow, Russia
[2] Institute of Problems of Chemical Physics, Russian Academy of Sciences, 142432 Chernogolovka, Moscow region, Russia
[3] Mining Institute, Ural Branch of the Russian Academy of Sciences, Sibirskaya str., 78a, 614007 Perm, Russia
[4] Kazakh National Research Technical University, Satpaev str., 22a, 050013 Almaty, Kazakhstan
[5] Department of Crystallography, St Petersburg State University, Universitetskaya Nab. 7/9, 199034 St Petersburg, Russia

ABSTRACT

The borate mineral satimolite, which was first described in 1969 and remained poorly-studied until now, has been re-investigated (electron microprobe analysis, single-crystal and powder X-ray diffraction studies, crystal-structure determination, infrared spectroscopy) and redefined based on the novel data obtained for the holotype material from the Satimola salt dome and a recently found sample from the Chelkar salt dome, both in North Caspian Region, Western Kazakhstan. The revised idealized formula of satimolite is $KNa_2(Al_5Mg_2)[B_{12}O_{18}(OH)_{12}](OH)_6Cl_4·4H_2O$ ($Z = 3$). The mineral is trigonal, space group $R\bar{3}m$, unit-cell parameters are: $a = 15.1431(8)$, $c = 14.4558(14)$ Å and $V = 2870.8(4)$ Å^3 (Satimola) and $a = 15.1406(4)$, $c = 14.3794(9)$ Å and $V = 2854.7(2)$ Å^3 (Chelkar). The crystal system and unit-cell parameters are quite different from those reported previously. The crystal structure of the sample from Chelkar was solved based on single-crystal data (direct methods, $R = 0.0814$) and the structure of the holotype from Satimola was refined on a powder sample by the Rietveld method ($R_p = 0.0563$, $R_{wp} = 0.0761$ and $R_{all} = 0.0667$). The structure of satimolite is unique for minerals. It contains 12-membered borate rings $[B_{12}O_{18}(OH)_{12}]$ in which BO_3 triangles alternate with $BO_2(OH)_2$ tetrahedra sharing common vertices, and octahedral clusters $[M_7O_6(OH)_{18}]$ with $M = Al_5Mg_2$ in the ideal case, with sharing of corners between rings and clusters to form a three-dimensional heteropolyhedral framework. Each borate ring is connected with six octahedral clusters: three under the ring and three over the ring. Large ellipsoidal cages in the framework host Na and K cations, Cl anions and H_2O molecules.

Keywords: satimolite, borate mineral, aluminium chloroborate, crystal structure, evaporite deposit, Satimola salt dome, Chelkar salt dome, Western Kazakhstan.

Introduction

Satimolite was discovered at the Satimola salt dome in the North Caspian Region, Western Kazakhstan. This mineral was first found by one of the authors of this paper (V.M.B.) in 1964 in cores of boreholes drilled for boron prospecting. For the holotype satimolite, quantitaive chemical analysis, powder X-ray diffraction (XRD) pattern, infrared (IR) spectrum, thermogravimetric data, measured density and optical characteristics were obtained. These data unequivocally demonstrate individuality of the mineral, the first aluminium borate found in sedimentary rocks (Bocharov *et al.*, 1969; Ostrovskaya, 1969).

The fine-grained character of satimolite aggregates made single-crystal XRD impossible, and the

absence of related minerals or synthetic compounds prevented acquisition of reliable crystal information even by analogy. Based upon only the powder XRD data (Table 1, # 1), the following orthorhombic unit cell was obtained: $a = 12.62$, $b = 18.64$, $c = 6.97$ Å and $V = 1639.6$ Å^3 (Bocharov *et al.*, 1969). Wet chemical analysis (Table 2, # 1) was performed from a 100 mg sample. Ostrovskaya (1969) supposed that the analysed material was polluted by Fe-bearing boracite, $(Mg,Fe)_3B_7O_{13}Cl$, and subtracted Mg, Fe and corresponding amounts of B, O and Cl from the analytical data. After the re-calculation of the result for 100 wt.%, the following composition was obtained: Na_2O 7.21, K_2O 6.06, Al_2O_3 24.10, B_2O_3 24.76, H_2O 28.03, Cl 12.70, $-O = Cl$ –2.86, total 100.00 wt.%. This corresponds to the following empirical formula calculated on the basis of 6 Cl apfu: $H_{52.10}K_{2.15}Na_{3.90}Al_{7.92}B_{11.91}O_{55.82}Cl_6$. Based on these data, the simplified formula $KNa_2Al_4B_6O_{15}Cl_3 \cdot 13H_2O$ ($Z = 2$) was suggested for satimolite. The discrepancy between measured and calculated density values, 2.10 and 1.70 g cm^{-3}, respectively, was explained by the possible presence of admixed boracite, a mineral with density of 2.7–3.0 g cm^{-3} (Bocharov *et al.*, 1969; Ostrovskaya, 1969). However this would require the presence of at least 30% of boracite impurity in the satimolite sample studied that is in contradiction with microscopic observations reported in the above-cited publications, as well as with our new data showing that the holotype sample of satimolite is almost pure.

No other original data on satimolite were published after 1969 until 2016, when this mineral was identified by the authors of the present paper (O.V.K. and I.I.C.) in a drillcore from the Chelkar salt dome in the same North Caspian Region, Western Kazakhstan (Korotchenkova and Chaikovskiy, 2016). Satimolite crystals suitable for the single-crystal XRD study and the crystal-structure determination were extracted from this sample. Along with the Chelkar satimolite, we have re-investigated the holotype material from Satimola. Characteristics of both samples turned out to be very similar, which allowed us to redefine satimolite, with the incorporation of the new crystallographic data, crystal structure and chemical formula.

Occurrence and general appearance

At Satimola, satimolite typically occurs as nodules (Fig. 1) up to 8 mm across included in clay–polyhalite–halite, clay–boracite–polyhalite and, rarer, clay–kiserite–polyhalite or clay–halite–kaliborite–polyhalite rocks. The mineral is mainly

concentrated in clay-enriched areas of the rocks. It also fills, together with halite and boracite, cracks in clay–polyhalite–halite and polyhalite–magnesite rocks. In all cases satimolite forms fine-crystalline, chalk-like snow-white aggregates (Bocharov *et al.*, 1969). They consist of well-shaped rhombohedral crystals up to 10 µm across (Fig. 2a). The content of mineral impurities in the satimolite aggregates studied does not exceed 1–3 vol.%. They are represented mainly by tiny halite and clay particles.

At Chelkar, satimolite was found in halite and sylvite–halite rocks with anhydrite and boracite (Korotchenkova and Chaikovskiy, 2016). It occurs as isolated, perfect in shape or blocky rhombohedral crystals up to 0.1 mm across, their clusters and nodules up to 0.5 mm, rarely up to 1.5 mm in diameter (Figs 2b–d). Separate crystals are colourless and transparent, with strong vitreous lustre, while nodules are white and translucent.

Chemical composition

The chemical composition of satimolite from both localities was studied using a JEOL JSM-6480LV scanning electron microscope equipped with an INCA-Wave 500 wavelength-dispersive spectrometer (Laboratory of Analytical Techniques of High Spatial Resolution, Dept. of Petrology, Moscow State University). The wavelength dispersive spectrometer mode was used, with an acceleration voltage of 20 kV and a beam current of 10 nA; the electron beam was rastered to 5 µm x 5 µm area to minimize sample damage. The standards used are as follows: microcline (K), NaCl (Na and Cl), wollastonite (Ca and Si), MgO (Mg), Mn (Mn), Al_2O_3 (Al), Fe (Fe) and FeS_2 (S). Contents of other elements with atomic numbers higher than oxygen are below detection limits. The presence of a significant amount of chlorine in satimolite prevents the quantitative determination of boron by electron microprobe due to the overlap of X-ray emission lines of the K series of B with L lines of Cl. It was not possible to determine H_2O because of the paucity of pure material.

Electron microprobe data for the samples studied by us are given in Table 2 in comparison with original, wet chemical data for the holotype satimolite. We have calculated the empirical formulae of our samples (No.s 2 and 3 in Table 2) on the basis of Al + Fe + Mg + Mn + Si = 7 apfu because these constituents: (1) are reliably determined by electron microprobe; and (2) fully occupy the Al sites in the crystal structure of satimolite (see below). Contents of B and

TABLE 1. Powder X-ray diffraction data for satimolite.

Satimola: holotype (Bocharov et al., 1969)		Satimola: holotype (our data)				Chelkar (our data)				
I_{obs}	d_{obs}, Å	I_{obs}	d_{obs}, Å	I_{calc}	d_{calc}, Å	I_{obs}	d_{obs}, Å	I_{calc}	d_{calc}, Å*	hkl
90	9.5	**100**	**9.72**	100	9.713	**100**	**9.65**	100	9.689	101
30	7.5	23	7.58	11	7.572	11	7.55	10	7.570	110
90	6.3	**45**	**6.34**	44	6.330	**42**	**6.28**	18	6.304	012
		8	6.01	0.5	5.972			0.1	5.965	021
		10	4.858	4	4.856			5	4.844	202
		12	4.825	7	4.818	8	4.797	5	4.793	003
40	4.66	23	4.690	14	4.689	19	4.674	7	4.685	211
30	4.46	10	4.374	4	4.371	4	4.362	3	4.370	300
90	4.01	**40**	**4.068**	50	4.065	**40**	**4.041**	38	4.050	113
20	3.84	6	3.787	0.25	3.786	2	3.782	0.5	3.785	220
		7	3.528	3	3.527			3	3.526	131
90	3.51	20	3.488	21	3.484	18	3.465	11	3.467	104
		46	**3.239**	8, 48	3.249, 3.237	**51**	**3.223**	3, 26	3.245, 3.230	312, 033
100	3.20	**65**	**3.199**	55	3.197	**67**	**3.194**	36	3.196	401
		6	3.165	3	3.165	4	3.148	4	3.152	024
40	2.98	14	2.980	4, 13	2.986, 2.976	14	2.969	3, 6	2.983, 2.971	042, 223
		5	2.947	0.25	2.946			0.5	2.944	321
40	2.83	13	2.864	7	2.862	10	2.858	4	2.861	410
		8	2.826	6	2.823	4	2.811	2	2.809	015
		5	2.780	3	2.778	3	2.773	2	2.775	232
		4	2.648	2	2.645	2	2.637	1	2.634	205
		9	2.582	6	2.581	6	2.578	4	2.580	051
		4	2.527	2	2.524	1	2.520	1	2.523	330
80	2.441	**28**	**2.465**	19, 14	2.466, 2.461	**26**	**2.459**	14, 9	2.464, 2.457	502, 143
20	2.419	12	2.430	14	2.428	13	2.421	8	2.422	404
		6	2.345	5	2.344	4	2.340	2	2.343	422
50	2.345	10	2.326	9	2.325	7	2.322	4	2.324	511
		6	2.314	3	2.312	3	2.302	2	2.307	324
		3	2.265	2	2.263			1	2.256	315

TABLE 1. (*contd.*)

Satimola: holotype (Bocharov *et al.*, 1969)		Satimola: holotype (our data)				Chelkar (our data)				
I_{obs}	d_{obs}, Å	I_{obs}	d_{obs}, Å	I_{calc}	d_{calc}, Å	I_{obs}	d_{obs}, Å	I_{calc}	d_{calc}, Å*	*hkl*
10	2.236	5	2.237	3	2.236	3	2.232	2	2.233	333
		3	2.188	0.5	2.186			0.25	2.185	600
		3	2.169	1	2.168			0.25	2.162	045
		11	2.124	13	2.123	11	2.117	8	2.119	054
50	2.103	7	2.101	5, 5	2.110, 2.100	9	2.101	3, 4	2.101, 2.100	036, 520
10	2.031	4	2.067	2	2.066	2	2.065	1	2.065	342
		7	1.991	4	1.991			4	1.988	603
80	1.966	21	1.974	32, 6	1.973, 1.970	20	1.968	18, 3	1.970, 1.960	514, 027
70	1.940	14	1.944	25	1.943	17	1.938	15	1.938	505
		5	1.927	0.5, 3	1.927, 1.925			0.25, 1	1.926, 1.923	612, 523
		3	1.910	0.5	1.906			0.5	1.898	217
		3	1.893	1	1.893	2	1.892	1	1.893	440
		3	1.884	0.5	1.882	1	1.880	0.5	1.877	425
		3	1.859	1	1.858	2	1.856	1	1.857	701
30	1.837	5	1.845	5	1.843	4	1.838	4	1.837	416
		4	1.828	4	1.826	3	1.826	2	1.822	155
30	1.798	6	1.805	6	1.804	5	1.804	4	1.804	621
		3	1.796	2	1.796			2	1.789	137
20	1.753	5	1.763	0.5, 3	1.764, 1.762	3	1.761	0.25, 3	1.763, 1.760	262, 443
				1	1.737	2	1.735	1	1.737	710
20	1.730	3	1.730	4	1.728	2	1.727	3	1.725	345
		2	1.700	0.25, 1	1.703, 1.698	1	1.700	0.1, 0.25	1.696, 1.690	327, 128
50	1.665	5	1.666	3, 5	1.668, 1.663	3	1.664	2, 3	1.668, 1.661	541, 704
60	1.612	6	1.622	9, 4, 4	1.623, 1.619, 1.618	6	1.616	4, 3, 1	1.617, 1.615, 1.611	057, 066, 318
		2	1.593	0.5, 0.5	1.599, 1.592			0.25, 0.25	1.598, 1.592	802, 271
		2	1.566	0.5	1.572			0.25	1.570	075
		2	1.564	0.25	1.563	1	1.560	0.25	1.562	363
10	1.552	2	1.555	2	1.553	1	1.549	1	1.548	517
		3	1.524	0.5, 3	1.526, 1.523			0.5, 1	1.526, 1.521	811, 544
60	1.508	9	1.515	14	1.514	8	1.515	9	1.514	550
		3	1.497	2	1.496	1	1.496	1	1.496	461
		2	1.489	4	1.488	1	1.485	3	1.583	508

2	1.477	2	3	1.473	1.473	2	1	1.472	642
		3	5	1.446	1.445	3	3	1.444	553
20	1.437	2	2, 0.5	1.427	1.434, 1.426	2	1, 0.25	1.429, 1.424	158, 805
		2	0.25, 2	1.411	1.413, 1.409	2	0.25, 1	1.411, 1.406	814, 176
20	1.395	3	0.25, 6	1.403	1.401, 1.401	3	0.5, 3	1.399, 1.395	725, 149
		3	1, 3	1.389	1.389, 1.388	1	0.5, 1	1.388, 1.384	464, 357
10	1.375		0.25		1.372		0.25	1.371	823
10	1.361	3	3	1.370	1.369	2	3	1.368	191
40	1.347	4	6	1.351	1.351	3	5	1.350	562
10	1.326	2	2	1.326	1.326	1	1	1.326	381
20	1.300	2	2	1.304	1.303	2	2	1.300	547
10	1.282	2	1, 1, 2	1.286	1.290, 1.287, 1.285	2	1, 0.5, 2	1.290, 1.287, 1.284	0.10, 2, 921, 194
10	1.264	2	0.5, 2	1.269	1.270, 1.266	2	0.25, 1	1.264, 1.261	1.2, 11, 0.5, 10
30	1.242	2	1	1.248	1.249	2	1	1.248	384

The strongest reflections for both samples studied by us are highlighted in boldtype. *Calculated for unit-cell parameters obtained from single-crystal data.

H_2O for these samples were calculated by stoichiometry, based on the structure data: for 12 B apfu and $(OH)_{18}(H_2O)_4$ pfu. For the original wet chemical analysis, with measured contents of all constituents, the formula was calculated on the basis of B + Al + Fe + Mg = 19 apfu (No. 1 in Table 2), i.e. for the sum of all constituents that fully occupy the B and Al sites. Iron is considered in our samples as Fe^{3+} by analogy with the original satimolite in which the trivalent state of Fe was determined directly by wet chemical analysis (Ostrovskaya, 1969).

Data reported in Table 2 show that in terms of chemistry, satimolite samples from Satimola (both original and new analyses) and Chelkar are close to each other and to the composition corresponding to the idealized formula $KNa_2(Al_5Mg_2)[B_{12}O_{18}(OH)_{12}](OH)_6Cl_4 \cdot 4H_2O$ ($Z = 3$) derived from the structure refinement data.

IR spectroscopy

In order to obtain IR absorption spectra, powdered samples were mixed with anhydrous KBr, pelletized, and analysed using an ALPHA FTIR spectrometer (Bruker Optics) with a resolution of 4 cm^{-1}; 16 scans were obtained. The IR spectrum of analogous pellet of pure KBr was used as a reference.

The IR spectra of satimolite samples from Chelkar and Satimola (Fig. 3) are close to each other and to the spectrum published by Ostrovskaya (1969). They contain bands in the regions 3000–3500 cm^{-1} (O–H-stretching vibrations), 1640–1660 cm^{-1} (bending vibrations of H_2O molecules), 1290–1450 cm^{-1} (asymmetric stretching vibrations of BO_3 triangles), 900–1200 cm^{-1} (stretching vibrations of BO_4 tetrahedra), 790–840 cm^{-1} (Al···O–H bending vibrations) and 694–696 cm^{-1} (bending vibrations of BO_3 triangles). Assignment of the bands with frequencies below 650 cm^{-1} is ambiguous: these absorptions are due to mixed lattice modes involving bending vibrations of BO_4 tetrahedra and Al···O-stretching vibrations, as well as librational vibrations of H_2O molecules. The observed splitting of the bands of B–O-stretching vibrations reflects the distortion of BO_3 triangles and BO_4 tetrahedra.

X-ray crystallography and crystal-structure determination data

Powder X-ray diffraction data for satimolite from Chelkar (Table 1) were obtained with a Rigaku

TABLE 2. Chemical composition and density of satimolite.

Analysis	1	2	3	4
wt. %				
Na_2O	4.97	5.05	4.57	5.14
K_2O	4.18	5.04	4.94	3.90
CaO	–	–	0.05	
MgO	8.39	7.76	6.84	6.68
MnO		–	0.11	
Al_2O_3	16.62	19.47	19.17	21.13
Fe_2O_3	1.78	0.72	1.38	
SiO_2		–	0.08	
SO_3		0.04	0.09	
Cl	11.48	12.23	12.63	11.75
B_2O_3	35.80	34.82*	33.77*	34.63
H_2O	19.33	19.51**	18.92**	19.42
$-O = Cl$	−2.59	−2.76	−2.85	−2.65
Total	99.96	101.88	99.70	100.00
Atoms per formula unit				
Na	1.92	1.96	1.82	2
K	1.06	1.28	1.30	1
Ca	–	–	0.01	
Mg	2.49	2.31	2.10	2
Mn		–	0.02	
Al	3.92	4.58	4.65	5
Fe^{3+}	0.27	0.11	0.21	
Si		–	0.02	
S		0.01	0.01	
Cl	3.88	4.14	4.41	4
B	12.32	12	12	12
O	17.805	17.925	17.845	18
OH	18	18	18	18
H_2O	3.855	4	4	4
Density (g cm^{-3})	2.10 (meas.)	2.12 (calc.)	2.15 (calc.)	
	2.08 (calc.)***			

1 – Satimola, holotype, wet chemical data (Ostrovskaya, 1969); 2 – Satimola, holotype, our electron microprobe data; 3 – Chelkar, our electron microprobe data; 4 – composition calculated for the idealized formula $KNa_2(Al_5Mg_2)[B_{12}O_{18}(OH)_{12}]$ $(OH)_6Cl_4 \cdot 4H_2O$.
*calculated for 12 B apfu; **calculated for $(OH)_{18}(H_2O)_4$ pfu; ***calculated using unit-cell parameters obtained by us. For analysis 1, with measured contents of all constituents, the formula is calculated on the basis of B + Al + Fe + Mg = 19 apfu, while for analyses 2 and 3, with calculated contents of B and H_2O, the formulae are calculated on the basis of Al + Fe + Mg + Mn + Si = 7 apfu. In all cases the amount of OH groups is fixed as 18 pfu and amount of O atoms is formally calculated from charge balance.
'–' = below detection limit.

R-AXIS Rapid II single-crystal diffractometer equipped with cylindrical image plate detector using Debye-Scherrer geometry (Co*K*α radiation, *d* = 127.4 mm).

Single-crystal XRD studies of the Chelkar satimolite were carried out using an Xcalibur S diffractometer equipped with a CCD detector. A full sphere of three-dimensional data was collected. Data reduction was performed using *CrysAlisPro*, version 1.171.37.34 (Agilent, 2014). The data were corrected for Lorentz factor and polarization effects. The mineral is trigonal, with the following unit-cell parameters: *a* = 15.1406(4), *c* = 14.3794(9) Å and *V* = 2854.7(2) Å^3. The crystal structure was solved by direct methods and refined in the space group *R*3̄*m* using the *SHELX-97* software package (Sheldrick, 2008) to *R* = 0.0814 for 597 unique reflections with *I* > 2σ(*I*). Hydrogen atoms of OH

FIG. 1. The holotype material from Satimola showing white nodules of satimolite in a brown-grey clay–polyhalite–halite rock. Field of view: 2.5 cm wide. Photo: N.A. Pekova.
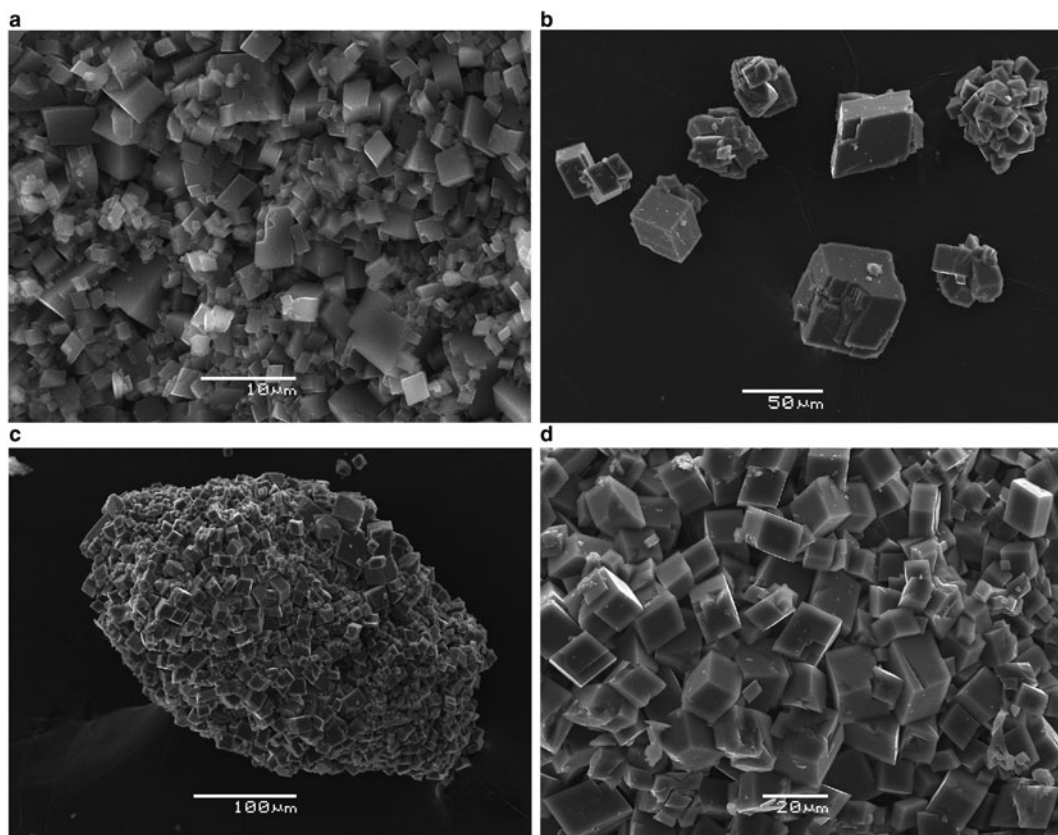

FIG. 2. Scanning electron image showing the morphology of satimolite crystals and aggregates from Satimola (*a*) and Chelkar (*b–d*).

groups were found in a difference-Fourier map and refined with O–H distances constrained to 0.90(1) Å. The crystal data and the experimental details for single-crystal experiment are presented in Table 3, atom coordinates, thermal displacement parameters and site occupancies in Table 4 (first line of each
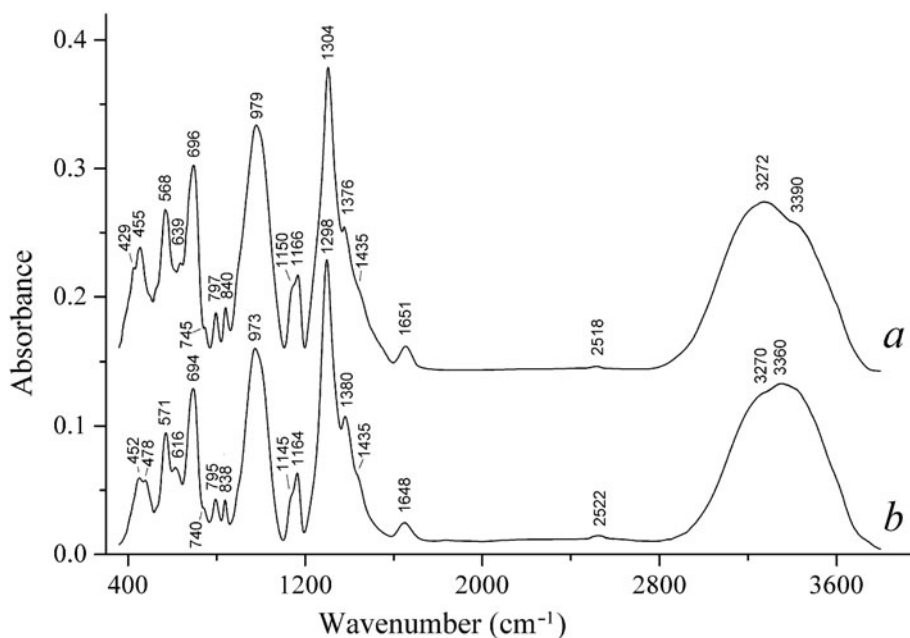
FIG. 3. Powder IR absorption spectra of satimolite from Chelkar (*a*) and Satimola (*b*).

row), selected interatomic distances in Table 5 and H-bond geometry in Table 6. Bond-valence calculations for fully occupied sites are given in Table 7. The crystallographic information file has been deposited with the Principal Editor of *Mineralogical Magazine* and is available as Supplementary material (see below).

The crystal structure of satimolite from Satimola (the holotype specimen) was refined on a powder sample by the Rietveld method, based on the structure model obtained from single-crystal XRD data for our sample from Chelkar. Powder X-ray diffraction data for the Satimola sample (Table 1) were collected using a computer-controlled STOE STADI MP powder diffractometer (Co$K\alpha_1$ radiation, $\lambda = 1.788965$ Å). A scan range of $5.00 \leq 2\theta \leq 119.48°$ was measured using a STOE linear position sensitive detector with exposure time of 500 s per 5$^{\rm o}$(2θ). Data treatment and the Rietveld structure analysis were carried out using the *JANA2006* program package (Petříček *et al.*, 2006). The profiles were modelled using a pseudo-Voigt function. The structure was refined in isotropic approximation of atomic thermal displacements. The refined unit-cell parameters of the sample from Satimola, $a = 15.1431(8)$, $c = 14.4558(14)$ Å and $V = 2870.8(4)$ Å^3, are close to

those obtained for the Chelkar satimolite (Table 3). Coordinates and thermal parameters of H atoms were not refined, thermal parameters of O (1), O(3), Ow(1) and Ow(2) and of mixed K and Cl sites were refined and fixed on the last stages of the refinement. Final agreement factors are: $R_{\rm p} = 0.0563$, $R_{wp} = 0.0761$ and $R_{\rm all} = 0.0667$. The observed and calculated powder XRD diagrams for satimolite from Satimola are shown in Fig. 4. Atom coordinates, thermal displacement parameters and site occupancies obtained for this sample are given in Table 4 (second line of each row).

All figures showing the satimolite structure are given according to single-crystal data for the Chelkar sample (Figs 5 and 6); the Satimola sample has, in general, the same structure.

Discussion

The crystal structure of satimolite (Fig. 5) is based on a three-dimensional heteropolyhedral framework built by 12-membered borate rings [B$_{12}$O$_{18}$(OH)$_{12}$] and octahedral clusters [M_7O$_6$(OH)$_{18}$] where $M =$ Al + Mg + Fe. Topologically the same framework was recently found in the crystal structure of synthetic borate PKU-8 with the formula written

TABLE 3. Crystal data, single-crystal data collection information and structure refinement details for satimolite from Chelkar.

Formula	$(\square_{0.68}Na_{0.32})_6(Cl_{0.68}K_{0.22}\square_{0.10})_6(Al_{0.66}Mg_{0.31}Fe^{3+}_{0.03})_7$ $[B_{12}O_{18}(OH)_{12}](OH)_6 \cdot 4H_2O$
Formula weight	1225.45
Temperature (K)	293(2)
Radiation and wavelength (Å)	Mo$K\alpha$; 0.71073
Crystal system, space group, Z	Trigonal, $R\bar{3}m$, 3
Unit cell dimensions (Å)	$a = 15.1406(4)$
	$c = 14.3794(9)$
V (Å^3)	2854.7(2)
Absorption coefficient μ (mm^{-1})	0.832
F_{000}	1839
Crystal size (mm)	$0.06 \times 0.08 \times 0.09$
Diffractometer	Xcalibur S CCD
Absorption correction	Multi-scan; empirical absorption correction using spherical harmonics, implemented in *SCALE3 ABSPACK* scaling algorithm.
θ range for data collection (°)	3.23–28.27
Index ranges	$-20 \leq h \leq 20, -20 \leq k \leq 20, -19 \leq l \leq 19$
Reflections collected	16,418
Independent reflections	882 ($R_{int} = 0.1750$)
Independent reflections with $I > 2\sigma(I)$	597
Structure solution	Direct methods
Refinement method	Full-matrix least-squares on F^2
Number of refined parameters	77
Final R indices [$I > 2\sigma(I)$]	$R_1 = 0.0814$, wR_2* $= 0.2115$
R indices (all data)	$R_1 = 0.1215$, wR_2* $= 0.2343$
GoF	1.114
Largest diff. peak and hole, e/Å^3	0.99 and –0.82

*$w = 1/[\sigma^2(F_o^2) + (0.1408P)^2 + 0.00P]$; $P = ([\text{max of } (0 \text{ or } F_o^2)] + 2F_c^2)/3$

as $(H_{18}Al_7B_{12}O_{36})Cl_3(NaCl)_{2.4}\cdot6.5H_2O$ (Gao *et al*., 2008). This compound is trigonal, with space group *R*3 and unit-cell dimensions $a = 15.0613(1)$ and $c = 14.0134(2)$ Å, that is very close to values found by us for satimolite. In the structure of the mineral there are two crystallographically non-equivalent octahedrally coordinated *M* sites labelled Al(1) and Al(2) (Table 4), and both sites are assumed to have an identical Al to Mg ratio close to 2:1 (with a small Fe admixture). This is in a good agreement with electron microprobe data (see Table 2 and footnote to Table 4). Six Al(1)O$_2$(OH)$_4$ octahedra encircle an Al(2)(OH)$_6$ octahedron sharing edges to form clusters (Fig. 6*a*) which could be considered as fragments of brucite-like layers. Two crystallographically non-equivalent B atoms are triangularly [B(1)] and tetrahedrally [B(2)] coordinated. B(1)O$_3$ triangles alternate with B(2)O$_2$(OH)$_2$ tetrahedra sharing common vertices and forming twelve-

membered borate rings (Fig. 6*b*). Each ring is connected with six octahedral clusters: three under the ring and three over the ring. Like PKU-8 (Gao *et al*., 2008), the framework of satimolite contains three-membered [2B + Al] rings. These units are known as a preferred geometry for the porous aluminoborate frameworks being crucial to stabilizing them (Gao *et al*., 2008; Ju *et al*., 2004 and references therein; Yang *et al*., 2007). In satimolite and PKU-8 these fundamental building units consist of one *M*-centred octahedron, one BO$_3$ triangle and one BO$_4$ tetrahedron. The same configuration was described recently in the structure of another synthetic borate PKU-3 (Chen *et al*., 2015). The remarkable feature of the aluminoborate frameworks of satimolite and PKU-8 is the presence of large ellipsoidal cages with an approximate size of 12 Å x 8.6 Å (Fig. 6*c*). In PKU-8 only two Cl sites matching with *A* site in the satimolite structure (*A* = Cl + K) and H$_2$O molecules were localized inside

TABLE 4. Atom coordinates and thermal displacement parameters (U_{eq}/U_{iso}, in Å^2), site occupancy factors (s.o.f.) and site multiplicities (Q) for satimolite. Single-crystal data for the Chelkar sample are given in the first line of each row and data for the holotype sample from Satimola (Rietveld refinement data) in the second line of each row.

Site	x/a	y/b	z/c	U_{eq}/U_{iso}	s.o.f.	Q
Al(1)[a]	⅓	−0.13391(12)	⅔	0.0214(6)	1	18
	⅓	−0.1319(7)	⅔	0.023(5)[b]		
Al(2)[a]	⅓	⅔	⅔	0.0250(11)	1	3
	⅓	⅔	⅔	0.022(11)[b]		
O(1)	0.26825(17)	−0.26825(17)	−0.2677(3)	0.0236(11)	1	18
	0.2683(7)	−0.2683(7)	−0.2698(10)	0.0103[b,c]		
H(1)	0.250(3)	−0.250(3)	−0.214(4)	0.08(4)[b]	1	18
	0.250	−0.250	−0.214	0.08[b]		
O(2)	0.6429(3)	−0.0713(3)	−0.2471(3)	0.0305(9)	1	36
	0.6456(10)	−0.0693(10)	−0.2448(9)	0.032(8)[b]		
H(2)	0.705(2)	−0.058(4)	−0.267(4)	0.049(18)[b]	1	36
	0.705	−0.058	−0.267	0.049[b]		
O(3)	0.0796(3)	−0.46021(17)	−0.2684(3)	0.0235(10)	1	18
	0.0789(14)	−0.4606(7)	−0.2675(15)	0.0125[b,c]		
O(4)	0.5792(3)	0.0074(3)	−0.1443(3)	0.0442(12)	1	36
	0.5763(11)	0.0080(11)	−0.1452(11)	0.047(7)[b]		
B(1)	0.0216(6)	−0.4892(3)	−0.1885(6)	0.0281(17)	1	18
	0.014(3)	−0.4930(15)	−0.198(2)	0.030(17)[b]		
B(2)	0.0	−0.3353(5)	½	0.0275(17)	1	18
	0.0	−0.3301(19)	½	0.029(17)[b]		
A	0.08132(9)	−0.08132(9)	−0.28791(18)	0.0506(8)	Cl$_{0.68}$K$_{0.22}$[c]	18
	0.0809(4)	−0.0809(4)	−0.2901(7)	0.0538[b,c]		
Na	0.5436(5)	0.0873(9)	−0.0093(6)	0.042(3)	0.32[c]	18
	0.5512(9)	0.1023(18)	−0.014(2)	0.060(11)[b]	0.33[d]	
Ow(1)	0.0	0.0	−0.3775(13)	0.045(5)	0.50[c]	6
	0.0	0.0	−0.423(4)	0.045[b,c]		
Ow(2)	0.5986(7)	0.1973(15)	−0.1155(14)	0.032(4)[b]	0.25[c]	18
	0.6020(14)	0.204(3)	−0.126(3)	0.052[b,c]	0.50[c]	
Ow(2')	0.5724(10)	0.145(2)	−0.0524(18)	0.046(6)[b]	0.25[c]	18
	–	–	–	–	–	

[a] Al(1) and Al(2) sites are considered as Al$_{0.66}$Mg$_{0.31}$Fe$_{0.03}$ taking into account electron microprobe data. The refined number of electrons in both sites is 13.08. [b] U_{iso}. [c] Fixed during the refinement. [d] Calculated from electron microprobe data, without taking into account the possible occurrence of a minor amount of H_2O.

the cage whereas in satimolite Na cations are also located inside the cages. The Na site in satimolite with partial occupancy [32% for sample from Chelkar and 33% for sample from Satimola] corresponds to one of the H_2O positions (Ow2) in PKU-8. If the *A* site in satimolite is occupied by Cl anions then this site could be included in the coordination sphere of Na cations with Na–Cl distance 2.949(8) Å. Moreover, Cl anions in the *A* site are involved in the formation of hydrogen bonds with H atoms of both crystallographically non-equivalent OH groups (Table 6): the Cl atom is bound with one H(1) cation and with two

H(2) cations with Cl–H distances of 2.43(6) and 2.23(2) Å, respectively (according to the single-crystal data for the Chelkar sample). The framework in PKU-8 is cationic, positively charged: $[H_{18}Al_7B_{12}O_{36}]^{3+}$ (Gao *et al.*, 2008), while the presence of Mg^{2+} replacing Al^{3+} in *M* sites in satimolite leads to significant decrease of the framework charge: *ca*. +0.7.

Structural data obtained by the Rietveld method for the holotype sample of satimolite from Satimola are very close to those found from single-crystal data for the Chelkar sample. The insignificant difference is in the content of ellipsoidal cages; in

TABLE 5. Selected interatomic distances (Å) in the structure of satimolite from Chelkar.

Al(1)–O(2)	1.908(4)×2	A(=K)–Ow(1)	2.491(10)
Al(1)–O(3)	1.913(3)×2	A(=K)–Ow(2')	2.713(18)×2
Al(1)–O(1)	1.999(3)×2	A(=K)–$Ow(2)$*	3.046(16)×2
<Al(1)–O>	1.940	A(=K)–O(2)	3.079(4)×2
		A(=K)–O(1)	3.225(5)
Al(2)–O(1)	1.950(4)×6		
<Al(2)–O>	1.950	Na–Ow(2)	2.10(2)
		Na–O(4)	2.484(8)×2
B(1)–O(4)	1.362(5)×2	Na–O(4)	2.779(11)×2
B(1)–O(3)	1.378(9)	Na–A(=Cl)	2.949(8)×2
<B(1)–O>	1.367		
B(2)–O(4)	1.437(5)×2		
B(1)–O(2)	1.480(6)×2		
<B(2)–O>	1.459		

* Two A(=K)–Ow(2) bonds are present only in the case when A–Ow(1) and A–Ow(2') bonds are absent.

the holotype sample no splitting of Ow2 site was observed and some H_2O can occur in the Na site.

According to the classification of fundamental building blocks (FBB) in borates (Burns *et al.*, 1995; Grice *et al.*, 1999), satimolite is a neso-dodecaborate with the FBB $6\Delta6\square = <\Delta\square\Delta\square\Delta\square\Delta\square\Delta\square\Delta\square>$. This FBB indicates that 12 boron polyhedra are involved in the formation of a 12-membered ring with alternating tetrahedra and triangles. Among minerals, 12-membered borate rings consisting of alternating tetrahedra and triangles were previously found in brianroulstonite, $Ca_3[B_5O_6(OH)_6](OH)Cl_2\cdot8H_2O$ (Grice *et al.*, 1997), where each ring shares three borate polyhedra with adjacent rings to form layers. In pringleite and ruitenbergite, two polymorphs of $Ca_9[B_{26}O_{34}(OH)_{24}]Cl_4\cdot13H_2O$ (Grice *et al.*, 1994), and in penobsquisite, $Ca_2Fe[B_9O_{13}(OH)_6]Cl\cdot4H_2O$ (Grice *et al.*, 1996), the dodecaborate rings are linked to form frameworks. Thus, satimolite is the first mineral with isolated 12-membered rings with alternating boron tetrahedra and triangles. It is interesting that all natural borates with such rings contain chlorine.

The structural formula obtained for the Chelkar sample is $(\square_{0.68}Na_{0.32})_6(Cl_{0.68}K_{0.22}\square_{0.10})_6$ $(Al_{0.66}Mg_{0.31}Fe^{3+}_{0.03})_7[B_{12}O_{18}(OH)_{12}](OH)_6\cdot4H_2O$ (Table 3), or $K_{1.32}Na_{1.92}(Al_{4.62}Mg_{2.17}Fe^{3+}_{0.21})_{\Sigma7}$ $[B_{12}O_{18}(OH)_{12}](OH)_6Cl_{4.08}\cdot4H_2O$. Though Mg^{2+} is not a predominant constituent in the Al sites it is an important charge-compensating cation that makes it necessary to include Mg in the idealized formula of satimolite, which can be written as

TABLE 6. Hydrogen-bond geometry (Å,°) in the structure of satimolite from Chelkar.

D–H⋯A	D–H	H⋯A	D⋯A	∠(D–H⋯A)
O(1)–H(1)⋯A(=Cl)	0.903(10)	2.43(6)	3.225(5)	148(9)
O(2)–H(2)⋯A(=Cl)	0.898(10)	2.23(2)	3.079(4)	158(5)

TABLE 7. Bond-valence calculations for fully occupied sites in the structure of satimolite from Chelkar.

	Al(1)	Al(2)	B(1)	B(2)	Σ*
O(1) = OH	0.40 ×2↓×2→	0.46 ×6↓			1.26
O(2) = OH	0.52 ×2↓		0.98	0.74 ×2↓	1.26
O(3)	0.51 ×2↓×2→		1.02 ×2↓		2.00
O(4)				0.84 ×2↓	1.86
Σ	2.86	2.76	3.02	3.16	

* The bond-valence sum for O(1) and O(2) presenting OH groups could be decreased if the hydrogen bonds with Cl⁻ as an acceptor are realized (Table 6) or insignificantly increased when K⁺ occupies the A site. The bond-valence sum for O(4) should be increased to 1.93 due to its participation in Na-centred polyhedron (Table 5). Bond-valence parameters were taken from Brese and O'Keeffe (1991).
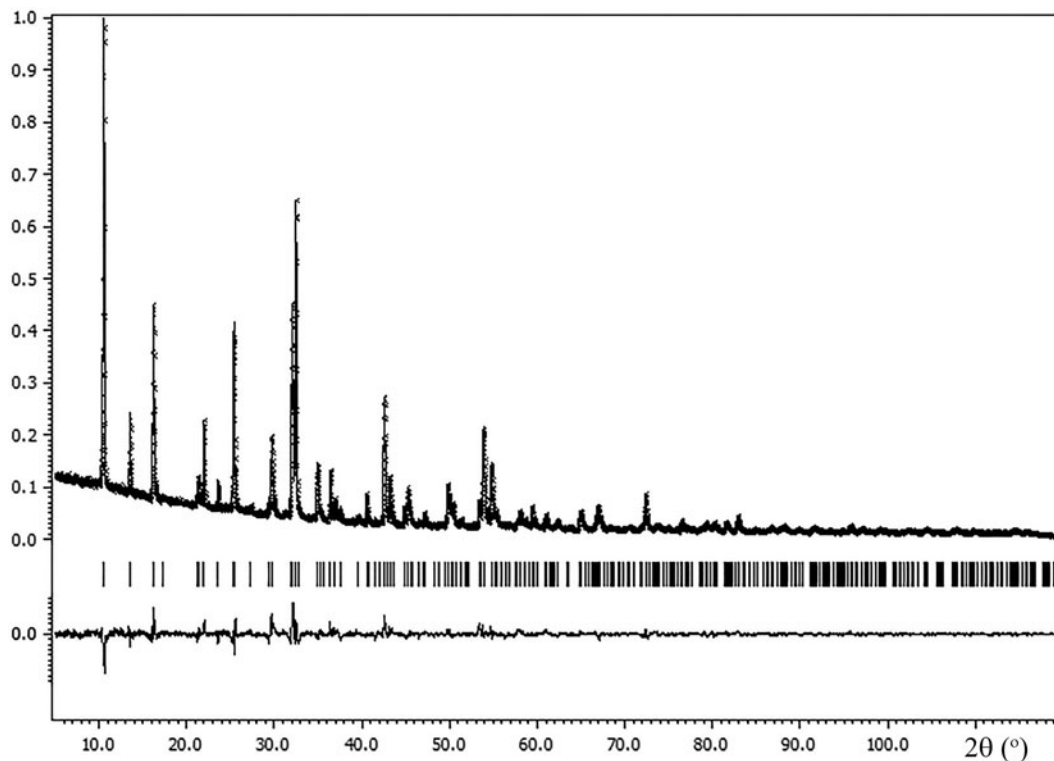
FIG. 4. Observed and calculated powder XRD patterns of satimolite from Satimola. The solid line corresponds to calculated data, the crosses correspond to the observed pattern and vertical bars mark all possible Bragg reflections. The difference between the observed and calculated patterns is shown at the bottom.

follows: $KNa_2(Al_5Mg_2)[B_{12}O_{18}(OH)_{12}](OH)_6Cl_4 \cdot 4H_2O$ ($Z = 3$). It corresponds to the chemical data for all the samples studied (Table 2).

By analogy with the mineral, the formula of a K- and Mg-free satimolite-related synthetic compound PKU-8, originally presented as $(H_{18}Al_7B_{12}O_{36})Cl_3(NaCl)_{2.4} \cdot 6.5H_2O$ (Gao *et al.*, 2008), can also be written as $Na_{2.4}Al_7[B_{12}O_{18}(OH)_{12}](OH)_6 Cl_{5.4} \cdot 6.5H_2O$.

Note that the initial chemical analysis of the holotype sample of satimolite from Satimola (No. 1 in Table 2: Ostrovskaya, 1969) corresponds well to the structural data obtained by us. It is also confirmed by good agreement between measured and calculated density values (Table 2) and by our calculations of the Gladstone-Dale compatibility index. Bocharov *et al.* (1969) reported that satimolite is optically biaxial, negative, with very small 2V value and the following refractive indexes: $\alpha = 1.535(2)$ and $\beta = \gamma = 1.552(2)$. We used these optical data for the compatibility index

calculation for the Satimola sample and found the following values of $1 - (K_P/K_C)$: –0.058 for the initial, wet chemical data and D_{meas}; –0.047 for the initial, wet chemical data and D_{calc}; –0.051 for our electron microprobe data and D_{meas}; and –0.041 for our electron microprobe data and D_{calc}. All these values correspond to the category 'good' (Mandarino, 1981). Optical data also confirm trigonal rather than orthorhombic symmetry of satimolite: it is probably a uniaxial mineral with a weak anomalous biaxiality.

Thus, the assumption by Ostrovskaya (1969) that the sample analysed was strongly polluted by boracite is definitely erroneous, as well as the formula based on this assumption, $KNa_2Al_4B_6O_{15}Cl_3 \cdot 13H_2O$, that was accepted for satimolite before the present work.

Powder X-ray diffraction data for satimolite from Satimola and Chelkar are close to each other and to the original powder XRD pattern of the mineral reported by Bocharov *et al.* (1969). Good agreement between measured and calculated powder
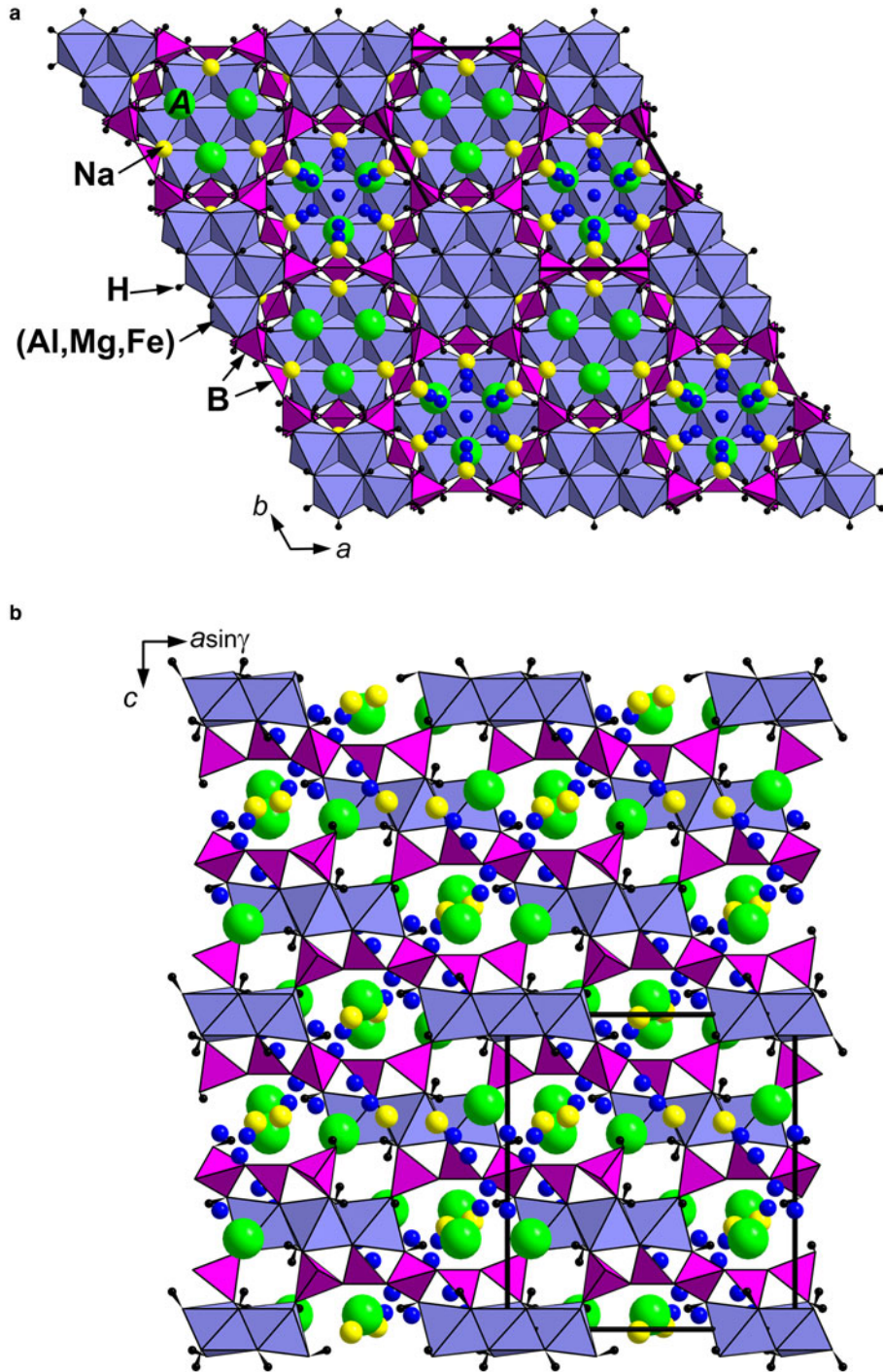
FIG. 5. The crystal structure of satimolite projected along c (*a*) and b (*b*) axes. Dark blue circles mark the positions of O atoms of H_2O molecules. The unit cell is outlined.
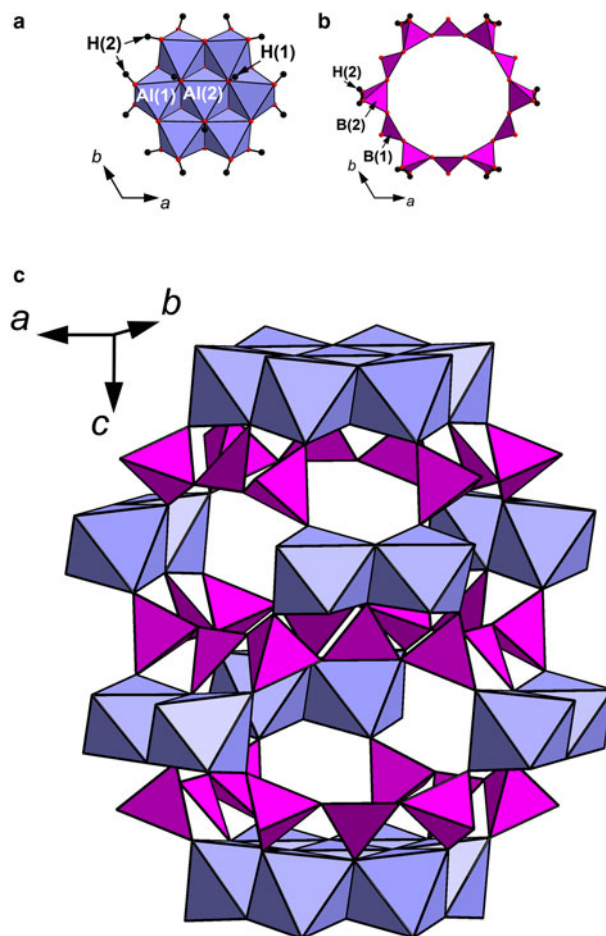
FIG. 6. Octahedral clusters (*a*); twelve-membered borate rings (*b*); and ellipsoidal cage (*c*) in the structure of satimolite.

XRD data allows us to give correct *hkl* indices (Table 1) that, consequently, differ from initially reported values based on a wrong unit cell.

Conclusion

The data obtained in this work for satimolite samples from two localities, including the holo-type, permit the present redefinition of satimolite. Its basic characteristics, namely chemical formula and crystal system have been significantly revised, the crystal structure was first solved and the powder XRD diagram has been refined and re-indexed. The novel results are in good agreement with all analytical data (wet chemical analysis, powder XRD pattern, measured density and optical characteristics) reported in original publications (Bocharov *et al*., 1969; Ostrovskaya, 1969).

Thus, satimolite is a trigonal (space group $R\bar{3}m$, $a = 15.14$ and $c = 14.38$–14.46 Å) hydrous chlor-oborate with the idealized formula $KNa_2(Al_5Mg_2)$ $[B_{12}O_{18}(OH)_{12}](OH)_6Cl_4 \cdot 4H_2O$ ($Z = 3$). In terms of crystal structure it has no analogues among minerals but is close to the synthetic borate PKU-8 $Na_{2.4}Al_7[B_{12}O_{18}(OH)_{12}](OH)_6Cl_{5.4} \cdot 6.5H_2O$ reported by Gao *et al*. (2008). The structure of satimolite contains a three-dimensional heteropolyhedral framework built by 12-membered borate rings $[B_{12}O_{18}(OH)_{12}]$ in which BO_3 triangles alternate with $BO_2(OH)_2$ tetrahedra sharing common vertices and octahedral clusters $[M_7O_6(OH)_{18}]$ with $M =$ Al_5Mg_2 in the ideal case. Each borate ring is connected with six octahedral clusters: three under

the ring and three over the ring. Large ellipsoidal cages in the framework host Na and K cations, Cl anions and H_2O molecules.

Acknowledgements

Supplementary material

To view supplementary material for this article, please visit https://doi.org/10.1180/minmag.2017.081.081

References

Agilent Technologies (2014) *CrysAlisPro Software system, version 1.171.37.34*. Agilent Technologies UK Ltd, Oxford, UK.

Bocharov, V.M., Khalturina, I.I., Avrova, N.P. and Shipovalov, Yu.V. (1969) A new mineral satimolite – hydrous chlorine-bearing borate of aluminium and alkalis. *New Data on Minerals of USSR* (*Proceedings of the Fersman Mineralogical Museum*), **19**, 121–126 [in Russian].

Brese, N.E. and O`Keeffe, M. (1991) Bond-valence parameters for solids. *Acta Crystallographica B*, **47**, 192–197.

Burns, P.C., Grice, J.D. and Hawthorne, F.C. (1995) Borate minerals. I. Polyhedral clusters and fundamental building blocks. *Canadian Mineralogist*, **33**, 1131–1151.

Gao, W., Wang, Y., Li, G., Liao, F., You, L. and Lin, J. (2008) Synthesis and structure of an aluminum borate chloride consisting of 12-membered borate rings and aluminate clusters. *Inorganic Chemistry*, **47**, 7080–7082.

Chen, H., Ju, J., Meng, Q., Su, J., Lin, C., Zhou, Z., Li, G., Wang, W., Gao, W., Zeng, C., Tang, C., Lin, J.,

Yang, T. and Sun, J. (2015) PKU-3: An HCl-inclusive aluminoborate for strecker reaction solved by combining RED and PXRD. *Journal of the American Chemical Society*, **137**(22), 7047–7050.

Grice, J.D., Burns, P.C. and Hawthorne, F.C. (1994) Determination of the megastructures of the borate polymorphs pringleite and ruitenbergite. *Canadian Mineralogist*, **32**, 1–14.

Grice, J.D., Gault, R.A. and Van Velthuizen, J. (1996) Penobsquisite: a new borate mineral with a complex framework structure. *Canadian Mineralogist*, **34**, 657–665.

Grice, J.D., Burns, P.C. and Hawthorne, F.C. (1997) Brianroulstonite: a new borate mineral with a sheet structure. *Canadian Mineralogist*, **35**, 751–758.

Grice, J.D., Burns, P.C. and Hawthorne, F.C. (1999) Borate minerals. II. A hierarchy of structures based upon the borate fundamental building block. *Canadian Mineralogist*, **37**, 731–762.

Ju, J., Yang, T., Li, G., Liao, F., Wang, Y., You, L. and Lin, J. (2004) PKU-5: An aluminoborate with novel octahedral framework topology. *Chemistry – A European Journal*, **10**, 3901–3906.

Korotchenkova, O.V. and Chaikovskiy, I.I. (2016) Boron minerals of the Chelkar deposit. *Problems of Mineralogy, Petrography and Metallogeny* (*P.N. Chirvinsky Scientific Conference, Perm University*), **19**, 55–65 [in Russian].

Mandarino, J.A. (1981) The Gladstone-Dale relationship. Part IV. The compatibility concept and its application. *Canadian Mineralogist*, **14**, 498–502.

Ostrovskaya, I.V. (1969) On the formula of a new mineral satimolite. *New Data on Minerals of USSR* (*Proceedings of the Fersman Mineralogical Museum*), **19**, 202–205 [in Russian].

Petříček, V., Dušek, M. and Palatinus, L. (2006) *Jana2006. Structure Determination Software Programs*. Institute of Physics, Praha, Czech Republic.

Sheldrick, G.M. (2008) A short history of SHELX. *Acta Crystallographica*, **A64**, 112–122.

Yang, T., Ju, J., Li, G., Liao, F., Zou, X., Deng, F., Chen, L., Su, J., Wang, Y. and Lin, J. (2007) Square-pyramidal/triangular framework oxide: synthesis and structure of PKU-6. *Inorganic Chemistry*, **46**, 4772–4774.